*Manuscript

Toxicity and potential risk assessment of a river polluted by acid mine drainage in the Iberian Pyrite Belt (SW Spain)

Aguasanta M Sarmiento[a,b*], Angel del Valls[a], José Miguel Nieto[b], María José Salamanca[b], Manuel Caraballo[a]

[a]Cátedra UNESCO/UNITWIN/WiCop, Departamento de Química Física, Facultad de Ciencias del Mar y Ambientales, Universidad de Cádiz, CP 11510 Puerto Real, Cádiz, Spain.
[b]Departamento de Geología, Universidad de Huelva, Campus 'El Carmen', CP 21071, Huelva, Spain

*E-mail address corresponding author: aguasanta.miguel@uca.es (Aguasanta M Sarmiento)

Abstract

The contamination of metals from acid mine drainage (AMD) is a serious problem in the southwest of the Iberian Peninsula, where the Iberian Pyrite Belt is located. This zone contains original massive sulphide reserves in order of 1700 Mt divided up in more than 50 massive sulphide deposits. Weathering of these minerals releases to the waters enormous amount of toxic elements which severely affect the sediments and surface waters of the region. The main goal of this paper is to evaluate the toxicity and the potential risk associated with the mining areas using Microtox test and different factors which assess the degree of contamination of the sediments and waters. For this, a natural stream polluted by AMD-discharge from an abandoned mine has been studied. The results show the elevated concentration of Cu, As and Zn involve an important potential risk on the aquatic environment, associated both in sediments and waters. Microtox test informs that the sediments are extremely or very toxic, mainly associated to concentrations of Fe, As, Cr, Al, Cd, Cu and Zn. Pollution is mainly transferred to the sediments increasing their potential toxicity. A natural creek affected by AMD can store a huge amount of pollution in its sediments and exhibits a not very low water pH and low water metal concentration.

Keywords: polluted river, heavy metals, toxicity, environmental risk

1. Introduction

Direct exposure to acid mine drainage (AMD) and sediments discharged from abandoned metal mine poses a serious hazard to aquatic biota, including to humans (Peplow and Edmonds, 2005). Large amounts of metallic ions and sulphate flowing into the streams imparted the typicall high acidity, high conductivity, etc., thereby resulting in the chemical degradation of the streams. Serious pollution hazards from AMDs have been reported in multiple sites worldwide. The studies show that AMD has a wide range of effects, viz, physicochemical changes in acidity, turbidity, sediment composition and ionic content. Also various biological impacts such as bioaccumulation, metabolic malfunctions (Blasco et al., 1999) and tissue damage affect the aquatic biota. AMD also reduces primary production and depleted numbers of sensitive species (Kim et al., 2002).

The contamination of AMD typically induces the formation of a significant amount of iron precipitates on the river bed, mainly as Fe oxy-hidroxy-sulphates precipitates (Bigham and Nordstrom 2000). The majority of elements of AMD discharging into aquatic system eventually end up in sediments that act as a sink of pollution, as well as a source of pollution (Delistraty and Yokel, 2007; Power and Champan, 1992). Whereas the total metal concentration is easier to measure in these environments, it is not a reliable indicator of toxicity due to distribution for contaminants among multiple phases varying in bioavailability (Landrum and Robbins, 1990) and speciation and partitioning effects, since different forms of chemical species in different compartments may vary widely in toxicity (Imai and Gloyna, 1990). Toxicity tests are desirable in sediment pollution evaluations because chemical and physical tests alone are not sufficient to assess potential effects on aquatic biota.

The Odiel River Basin (Fig. 1a) is generally recognized as a fluvial system with a catastrophic ecological situation due to chronic and severe pollution from AMD, so much so that it affects 37% of the length of the drainage network (Sarmiento et al. 2009a). The Odiel River drains the central part of the Iberian Pyrite Belt (SW Spain). This zone contains original massive sulphide reserves in the order of 1700 Mt divided up in more than 50 massive sulphide deposits. Pyrite, sphalerite, galena and chalcopyrite are the main mineral phases that make up these deposits, which also contain accessory amounts of As, Cd, Co, Ni, Cr, etc. Weathering of these minerals releases to the waters enormous amount of toxic elements which severely affect the Odiel River from its upper section to the Huelva Estuary (Cánovas et al. 2007; Olías et al. 2004; 2006a).

Other examples of rivers affected by AMD in the southwestern of Iberian Peninsula are several streams from the low part of the Guadiana Basin (Delgado et al., 2009; Grande et al., 2005), the Tinto River (Cánovas et al., 2008; 2010), etc. Apart from chronic pollution by AMD, major accidents, most often resulting from the breaching of an effluent retaining dike, can bring about major pollution incidents as in Andalusia (south-western Spain), where, in 1998, a dam breaking resulted in the contamination of the Guadiamar River (Grimalt et al., 1999; Olías et al., 2006b), an affluent of the Guadalquivir, which drains the Donana National Park (UNESCO world reserve).

Despite the high number of papers covering many environmental issues related with AMD pollution, a better study of water and sediment toxicity in this region is needed in order to evaluate the potential risk associated with the mining areas. The main goal of this paper was to determine metal toxicity to one aquatic bacterium (Vibrio fisheri) in typical AMD-sediments using Microtox test. Use of the commercial bioassay Microtox® like toxicity test has increased in recent years since its capacity to detect the ‘‘hot spots’’ of field contamination in the screening procedure (Mowat and Bundy, 2001; Stronkhorst et al., 2003; Van Beelen, 2003). Others studies on soils and rivers have used Microtox® to assess the impact of contamination by AMD (Boularbah et al., 2006; Guéguen et al., 2004). Also the environmental risk associated with the toxic metal total concentrations in waters and with their geochemical fractionation in sediment was evaluated.

2. Materials and methods

2.1. Site description

This work has been focused on a contaminated section of the Villar Creek, one of the main tributaries of the Odiel Basin. Villar Creek is polluted by the Tinto Santa Rosa mine, located in the central-east of Odiel Basin (Fig. 1a). This mining area contains a mine portal where the acid effluent emanates, in adition to large waste piles and tailings impoundments. As a result, a polluted AMD-watercourse flowing during 500 meters downstream is joined into the Villar Creek. Before joining, the Villar Creek has clean water (7.1 of pH, 129 mg l^{-1} of HCO_3^-, 48.4 mg l^{-1} of SO_4^{2-}; Sarmiento, 2008) (point V1, Fig. 1b) and after receiving the polluted water, this stream is severely spoiled and flows into the Odiel River a few kilometres downstream.

2.2. Water samples

2.2.1. Sampling and field measurements

Field work was performed on September 2007. Two water bodies were assessed in this study: (1) the polluted AMD-watercourse coming from the mine that flows downstream into (2) the Villar Creek. In both, four sampling points were studied: TR2, TR3, TR4, TR5 (Fig. 1b) belonging to the AMD-watercourse and V1, V6, V7, V8; (Fig. 1b) from the Villar Creek, being the point V1 at Villar Creek, located upstream (geochemical background) the mixture with waters from the AMD-watercourse. Flow rates have been calculated in both watercourses by conventional methods using digital flow meters (GLOBAL WATER).

Several physicochemical parameters were measured in the field. Temperature, pH and specific conductance were measured using a portable MX 300 meter (Mettler Toledo). Dissolved oxygen was analysed using a Hanna meter, and redox potential was determined using a Hanna meter with Pt and Ag/AgCl electrode (Crison). The pH meter was calibrated using Hanna standard solutions (pH 4.01 and pH 7.01) and redox potential was checked using Hanna standard solutions (240 mV and 470 mV). Gross alkalinity was measured in situ using CHEMetrics® Total Titrets®.

Water samples were filtered immediately in field through 0.22 µm Millipore filters fitted on Sartorius polycarbonate filter holders. Samples for cations and metal analysis were acidified in the field to pH<2 with HNO_3 (2%) suprapur. Samples collected for sulphate determinations were filtered but not acidified. Samples for Fe(II) determination were filtered through 0.1 µm, and the Fe(II) was complexed by adding 0.5 % (w/w) 1,10-phenanthroline chloride solution after buffering to pH=4.5 with an ammonium acetate/acetic buffer (Rodier et al., 1996). All the samples were stored in the dark at 4ºC in polyethylene bottles until analysis.

2.2.2. Chemical analysis

Concentrations of dissolved Al, As, Ba, Cd, Co, Cr, Cu, Fe, Mn, Ni, Pb, and Zn were determined by Inductively Coupled Plasma Atomic Emission Spectrometry (ICP-AES Jobin-Ybon Ultima2) using a protocol especially designed for AMD samples (Tyler et al., 2004). Analysis was performed at the Central Research Services of the University of Huelva. Multielement standard solutions prepared from single certified standards supplied by SCP SCIENCE were used for calibration. They were run at the beginning and at the end of each analytical series.

Certified Reference Material SRM-1640 NIST fresh-water-type and inter-laboratory standard IRMM-N3 wastewater test material, European Commission Institute for Reference Materials and Measurements, were also analysed. Detection limits were calculated by average, and standard deviations from ten blanks. Detection limits were less than 100 µg l^{-1} for Al, Fe and Mn; 50 µg l^{-1} for Zn, 5 µg l^{-1} for Cu and less than 1 µg l^{-1} for the other trace elements. Sulphate was determined by Ion Chromatography using a Dionex DX-120 machine fitted with an AS 9-HC of 4 x 250-mm column and a 4-mm ASRS-ULTRA suppressing membrane. Detection limit for SO_4^{2-} was less than 0.5 mg l^{-1}.

Fe(II) was determined using colorimetry at 510 nm with SHIMADZU UVmini-1240 spectrophotometer. The detection limit was 0.3 mg l^{-1} and the precision better than 5 %.

2.3. Stream sediments

For every sampling point, surficial fresh sediments (upper 5 cm) were collected and stored in acid-rinsed polyethylene bottles. The samples were refrigerated (4 ºC) and taken to the laboratory for analyses.

The sediment samples were air-dried at room temperature and ground into fine slurry using a quartz ball mill. Metals fractionation in the homogenized sediments was determined following the first four steps of a sequential extraction procedure proposed by Caraballo et al. (2009a) for the study of AMD precipitates in order to distinguish the elements associated with the bioavailable fractions (two first steps) of those associated with the non-mobile fractions (two last steps). The following four-step sequence was carried out for the sequential extraction: F1, water soluble fraction; F2, sorbed and exchangeable fraction; F3, poorly ordered Fe (III) oxyhydroxides and oxyhydroxysulphates; F4, highly ordered Fe(III) hydroxides and oxides. The extractants were analyzed by ICP-AES alike above and the detection limits were the same.

2.4. Data analysis

To evaluate the environmental risk different factors for the potentially toxic metals in the environment (As, Cd, Co, Cu, Pb, Ni, Cr, Zn) were included in the analysis. The index of geoaccumulation (*Igeo*), the environmental risk factor (*ERF*) and the degree of contamination (C_d), defined as,

$$Igeo = log_2 (C_n / 1.5\ B_n)$$

$$IRF = (C_n – C_{SQV}) / C_{SQV}$$

$$C_d = \Sigma C^i_f = (C^i_{0\text{-}1} / C^i_n)$$

The Index of geoaccumulation (*Igeo*) was introduced by Müller (1981) and used as a measure of metal pollution in sediments, where *Cn* is the toxic element concentration in a sample and *Bn* is the measured concentration of the element in unpolluted sediments. The factor *1.5* is used to compensate possible variations of the background data by lithogenic effects. This geochemical background was obtained from unpolluted sediments taken in a fresh natural stream belonging to the South-Portuguese Zone (values used to *Bn* in mg kg^{-1}: As 29; Cd 0.3; Cu 21; Pb 30, Zn 50. Data unpublished). Samples were classified from unpolluted (*Igeo*<1) to very highly polluted (*Igeo*>5).

The environmental risk factor (*ERF*) has been calculated for both sediment and water samples. It was used to establish those stations in which the toxic element concentrations are associated with an environmental risk (Riba et al., 2002). *Cn* is the dissolved element concentration measured in the water samples. For the sediments, *Cn* corresponds to the addition of the most mobile fractions (F1+F2). The term C_{SQV} represents the highest concentration of the studied element non-associated with biological effects. The C_{SQV} for the sediments are obtained from the site-specific quality values reported by Riba et al., (2004) (values used to C_{SQV} for sediments in mg kg^{-1}: As 27.4; Cd 0.51; Cu 209; Pb 206; Zn 513). The C_{SQV} for the waters were obtained from EPA's compilation of national recommended water quality criteria using the Criteria Continuous Concentration (CCC) as an estimate of the highest concentration of an element in surface water to which an aquatic community can be exposed indefinitely without resulting in an unacceptable effect (values used to C_{SQV} for waters in μg l^{-1}: Zn 120; Cd 0.25; Cu 9; Pb 2.5, As 150).

Hakanson (1980) proposed the contamination factor (C^i_f) in order to assess soil contamination by the use of reference concentrations in the surface layer of botton sediments corresponding to preindustrial activity. $C^i_{0\text{-}1}$ is the mean content of metals from al least five sampling sites and C_n^i is the preindustrial concentration of individual metal. In this work, we used the concentration of elements obtained from unpolluted sediments taken in a fresh natural stream belonging to the South-Portuguese Zone. The C^i_f is a single-element index and four categories are defined from low contamination factor indicating low contamination (C^i_f <1) to very high contamination factor

($C^i_f \geq 6$). The sum of contamination factor for all the elements examined represents the contamination degree (C_d) of the environment, and four classes are recognized: low degree of contamination (C_d<8); moderate degree of contamination ($8 \leq C_d < 16$); considerable degree of contamination ($16 \leq C_d < 32$) and very high degree of contamination ($C_d \geq 32$).

2.4.1. Geochemical modelling

Metal species concentrations were interpreted with the assistance of the equilibrium chemical-speciation/mass-transfer model PHREEQC (Parkhurst and Appelo, 1999). Analysed iron species were used to calculate *pe* and the thermodynamic database MINTEQA2 was employed (Allison et al., 1990).

2.4.2. Statistic analysis

In order to clarify the relationship between toxicity to Microtox and the composition of toxic elements from AMD-sediments, discriminatory and cluster analysis were performed to the data, including pH of the water samples, metal and sulphate concentration of the extracted from the most bioavailable fraction (F1) and toxicity test data. The first sequential extraction step was selected due to its resemblance with the dilution procedure in the Microtox test. The program used for cluster analysis operates by applying the Ward method or 'second-order central moment', which is a hierarchical method that calculates the mean of all the variables for each cluster; next it calculates the Euclidean distance between each factor and the mean of its group and then adds the distances from each case. In short, through the application of this technique, the variables studied can be classified into different 'categories'.

2.5. Microtox® bioassay

The commercial Microtox® test is a bioassay that uses the bioluminescence of the bacteria *Vibrio fischeri* as an indicator of the quality of the sample exposed; the bioluminescence of the bacteria is related to its metabolism therefore, a diminution of the sediment quality will be reflected in the decrease of the quantity of light emitted. In the Microtox® toxicity test, the measures of EC50 (which is the concentration of dry sediment that provokes a 50% inhibition of the light emitted by the bacteria) provide the information about the sediment toxicity. The bioassay of bioluminescence inhibition with the bacteria *V. fischeri* was conducted on solid phase with the commercial Microtox® apparatus (model 500) by following the protocols for the Basic Solid Phase Test (BSPT) according to the standard operating procedure (AZUR Environmental, 1998). Briefly, 7 g (±0.01 g) of sediment were tested as suspensions prepared with 35 mL of commercial Microtox® Solid Phase Test Diluent and diluted to a series of nine concentrations in the cuvettes. The reconstituted bacteria were added to the dilutions which were incubated for a period of 15 min at 15 ºC. The modification of the basic solid phase test (BSPT) reported by Campisi et al. (2005) was carried out and an average from three values of the EC50 was obtained for each sample.

3. Results and disscusion

3.1. Hydrogeochemical characteristics and evolution of the water samples along the watercourses

Figure 2a shows some physicochemical parameters measured in the field and figure 2b the several chemical processes occurring along the watercourses. The Minimum pH value and maximum electrical conductivity were 2.9 (TR5) and 3.3 mS cm^{-1} (TR3), respectively. The molar ratio of $Fe(II)/SO_4^{2-}$ theoretically obtained from the oxidation of pyrite is 0.5. Fig. 2b shows this ratio along the watercourses (triangle symbols), being close to 0.5 only in the first point where pyrite oxidation takes place. Along the AMD-watercourse (water flow of 3.5 l s^{-1}), Fe(II) is oxidated to Fe (III), so the Fe(II)/(III) ratio strongly decreases (Fig. 2b) while redox potential increases from 513 to 637 mV (Fig. 2a). Total Fe concentration also decreases being lesser than the theoretical concentration of Fe from the pyrite oxidation (Fe-py in Fig. 2b) due to oxyhidroxisulphate precipitation (Asta et al., 2010a). This precipitation originates a slight decreased of the pH from 3.2 to 2.9 (Fig. 2a), enhancing acid hydrolysis of bedrock minerals and increasing the concentration of elements such as Mn, Al, Ca, Mg, etc. Before joining, the clear water from the Villar Creek presents pH of 7.8, and concentrations of sulphate and bicarbonate of 48 and 130 mg l^{-1}, respectively. Once the AMD-watercourse flows into Villar creek (water flow of 69 l s^{-1}), pH increases considerably (from 2.9 to 5.2) and Fe and Al are massively removed. In adittion, and directly related with metal precipitation, electrical conductivity strongly decreases and the rest of elements are depleted in solution (Table 1) due to adsorption, coprecipitation and dilution processes. After total mixture, the main process occurring is the dilution (Fig. 2b).

Chemical composition of the AMD-watercourse presents extremes values up to 8400 mg l^{-1} of sulphates, 3.7 mg l^{-1} of As, 20 mg l^{-1} of Cu, 72 mg l^{-1} of Zn, 710 mg l^{-1} of Fe, and minor amounts of other elements (Table 1). The high acidity generated during the oxidising process enhances silicates hydrolysis in the spoiled materials, dissolving large quantities of their constituent elements such as Al (up to 80 mg l^{-1}), Mn (37 mg l^{-1}), etc. After joining with the uncontaminated stream, the pH of Villar Creek decreases from 7.8 to 4.8 (Fig. 2a) and concentrations of toxic elements such as As, Cd, Co Cr, Ni, Zn, Cu, etc. increase (Table 1).

The evolution of trace element concentrations downstream shows a similar pattern. It is known that trace metals concentration is commonly controlled by adsorption into mineral surfaces so the variations in the behaviour of these trace elements can be attributed to the different affinity of each aqueous species to the surface of the precipitates (Asta et al., 2010b). When Fe and Al precipitate, other metals can hence get adsorbed to them. Generally, metal concentrations decrease progressively downstream, but some differences can be observed. For example, in point V6 (pH of 4.8) most of the elements have high concentrations such as 53 μg l^{-1} of As, 128 μg l^{-1} of Co or 84 μg l^{-1} of Ni, and when the pH increases downstream (V7, pH of 5.2) trace elements concentration suffer a noticeable decrease (Table 1). However, some meters further downstream (V8 pH of 6.4), the concentration of these elements turn to be the same or slightly higher (as can be observed for Cr or Cd, Table 1). This phenomenon is possibly due to desorption processes as it will be discussed below.

3.2. Evolution in the sediment chemical composition along the water course

Sediment samples were undergone to a sequential extraction procedure specifically designed for AMD-precipitates in order to obtain a better understanding of the metal distribution. The results were grouped according to their bioavailability into: bioavailable fractions (F1+F2) and non-mobile fractions (F3+F4), fig. 3. The highest concentrations were found in the non-mobile fractions associated with the two steps of the sequential extraction specifically design to dissolved poorly ordered oxyhydroxydes and hydroxysulphates of Fe like schwertmannite or ferrihydrite (F3) and to dissolved more cristallyne Fe phases like goethite or jarosite (F4). Schwertmannite is the dominant phase that precipitates directly from AMD in the discharge from Tinto Santa Rosa Mine (Asta et al., 2010a), and makes up the loose sediments that will later form current consolidated terraces (Pérez-López et al., 2010). However, it was observed that in the current terraces, schwertmannite is gradually transformed into mainly goethite and eventually jarosite with depth (Asta et al., 2010a; Pérez-López et al., 2010). In these fractions maximums of up 338 g kg^{-1} of Fe, 5 g kg^{-1} of As, 2400 mg kg^{-1} of Cu or 1320 mg kg^{-1} of Zn can be found (Fig. 3). Although the concentration of toxic elements is lower in the most bioavailable fractions, these are the most hazardous and harmful for the environment consisting of exchangeable metals and those soluble in water or in slightly acidic conditions, showed maximums of up to 56 g kg^{-1} of Fe, 1870 mg kg^{-1} of Cu, 900 mg kg^{-1} of Zn, 355 mg kg^{-1} of As, etc., in these fractions (Fig. 3).

The high efficiency of Fe precipitates sequestering arsenic has been study in this region by previous studies (Asta el al., 2010a, b). As can be observed, Fe and As concentrations in both bioavailable and non-mobile fractions show a coupled decreasing tendency in two sections, along the AMD-watercourse and along the Villar Creek (Fig. 3). The massive Fe precipitation is induced when the AMD-watercourse joins the Villar River (point V6), involving a noticeably increase of Fe and As content in the sediments. However, a considerable quantity of both elements is observed in the bioavailable fractions after joining. Aluminum, Cu and Zn distribution in the sediments clearly reflects the pH-dependent removal of those elements (Fig. 3). Aluminum precipitation takes place only after water pH reachs a value of 5 (Bigham and Nordstrom, 2000) and coupled removal of Cu and Zn in the Al-precipitates have been reported in many studies (Caraballo et al., 2009b). At the first point of the mixing zone (V6) water pH is lower than 5 (Fig. 2) and the amount of Al, Cu and Zn in the sediments is equivalent to the one observed in the sediments along the AMD-watercourse. When water pH is higher than 5 (V7 and onward) the massive precipitation of Al and the coupled removal of Cu and Zn can easily be observed (Fig. 3). The higher concentration of Cu and Zn in the last sampling point (V8) can be explained by adsorption of these elements in the higher available Al-precipitates. Bioavailability of those three elements is almost negligeable in the AMD-precipitates and increase remarkeably in Villar Creek sediments. Cobalt, Cd, and Ni do not show a clear trend in the sediments, however can be observed how the highest concentration for the bioavailable fractions correspond to the last sediment samples at Villar Creek (Fig. 3). Lead concentration in water is almost completely removed before joining with the Villar Creek (Table 1) and therefore the concentration of this element in the river sediments is nearly indiscernible. Cr concentration in the sediments does not exhibit a clear trend and it can be observed in some extend in all the samples.

3.3. Environmental risk and toxicity

As described above, the concentration of some toxic elements in the sediments increases after the join with the natural river (Villar Creek, fig. 1) in the most bioavailable fractions and also in the water, possibly due to desorption processes. Elements with the capacity of forming oxyanions, such as Cr and As, undergo different behaviours when are adsorbed to some mineral phases. For example, As(V) is especially well known to be adsorbed onto schwertmannite (Asta el al. 2010b), whereas As(III) seems to be less strongly adsorbed to this mineral phase. The sorption of these species depends on several factors, including Fe concentration and pH (Roussel et al, 2000), Fe solubility (Asta et al., 2010b), photooxidation processes (Sarmiento et al., 2007), etc. Sarmiento et al. (2009b) studied the evolution of the inorganic arsenic species along the watercourse of the Odiel River, reporting a increase for As(III/V) ratios downstream. On the other hand, under low pH conditions Cr(III) appears as free specie which is quickly oxidizeded to Cr(VI) as $Cr_2O_7^{2-}$. Both of them are rapidly adsorbed onto Fe precipitates. However, when the pH increases (pH 5-6), Cr(VI) can ungergoes desorption processes due to colloids surface charge (Zanker et al., 2002). To asses the speciation of As and Cr and subsequently their potential water toxicity, the hydrogeochemical modelling PHREEQC was employed. Fig. 4 shows the As(III)/(V) and Cr(IV)/(III) ratios increase along the watercourse as a result of an increase of pH. As mention above, the most toxic species are As (III) and Cr(VI), therefore, although the total concentration of these elements is low, the toxicity and risk to aquatic biota is potentially high, both in sediments and waters.

Geoaccumulation index has been used to assess the metal pollution of sediment samples compared with the metal baseline levels of the area. The evolution of this index along the watercourse is showed in fig. 5 for As, Cd, Cu, Pb and Zn. It can be observed, all the sampling points are subjected to serious pollution effect with regard to As and Cu, (average *Igeo*>3) corresponding to the strongly polluted class. Lead can be considered as a strongly polluted in the first point close to the contaminant source, although after this point the pollution with regard to Pb decreases until joining with the unpolluted water, where it increases again. The Igeo increases for all the elements (except for arsenic) after joining with the natural water. Along this creek, all these elements have an *Igeo* corresponding to the range between moderately and extremely polluted classes. However, over the entire watercourse, the *Igeo* with regard to Co, Cr and Ni is below zero, belonging to the unpolluted class.

The assessment of the overall contamination of sediment based on the degree of contamination (C_d) for the mean metal contents was 130 (Table 2) indicating very high degree of contamination (Hakanson, 1980). The minimum value of the contamination degree (C_d = 108, belonging to sample TR5) also denoted very high degree of contamination. The sediment sample more polluted was taken in the point V8 (C_d = 281) belonging to the stream after the join. According to the contamination factor (C^i_f) values the sediment was classified as slightly contaminated with Co, Cr and Ni, moderately contaminated with Cd and Pb and heavily contaminated with Cu, Zn and specially arsenic. This last contributed to the extent index of sediment contamination by 73%.

To establish the potential risk effects caused by some toxic elements on the aquatic environment, the ERFs were calculated for water and sediment samples and plotted in fig. 6. The positive values of the factors inform about a potential adverse biological effect associated with the metals. For water samples belonging to the AMD-watercourse, the high ERFs are mainly associated with Zn, Cd and Cu, presenting values higher than 100. Samples from the Villar Creek present values below but close to zero for As and Pb and higher than 20 for the rest of the studied elements. For sediment samples, the ERFs have negative values (close to zero) along the acid watercourse for Cd, Zn, Cu and Pb, changing to positive values after joining with the creek. On the contrary, the ERF for arsenic shows an inverse trend decreasing from high positive values along the AMD-watercourse to negative values after joining with the creek.

Table 3 shows the EC50 results obtained through the Microtox® test with the sediments collected along the watercourses. To categorize the studied sediments it was decided to use the classifications rated by Brouwer et al. (1990), Bennett and Cubbage (1992) and Kahru et al. (2000). The sediment sample from upstream area showed EC50 of 783 mg l^{-1} (1.29%, 77.7 TU), and can be reported as slightly or very toxic to Microtox (Table 3). The toxicity of the sediments along the AMD-watercourse (from TR3 to TR5) has a quite steady trend with values of 0.28%, 358 TU corresponding to very toxic or extremely toxic class. The first sample after joining with the natural river (V6, fig. 1) exhibits a noticeable decrease in the EC50 (83 mg l^{-1}) that implies an extremely toxic environment (0.14%, 733 TU) in both classifications employed. The last point sampled (V8), where concentrations of Al, Cd, Cu, Ni, Co and Zn have been observed to be quite high in the most bioavailable fractions (Fig. 3), the sediments can be classified as very toxic to Microtox (0.34%, 29% TU).

The groupings in Fig. 7 show the variables ordered in similar clusters, while the distances between the points on the horizontal axis represent the order of affinity or proximity. Moreover, in this figure we can see how each parameter fits in with successive clusters as they form. The measured parameters form two main clusters. On the left side of the dendogram, a first level of aggregation is established with the pair Fe – UT which, at the same time, is associated with SO_4^{2-}. Finally, the pair As – Cr forms a cluster with the previous. A second cluster, on the right side of the dendogram, shows a first level of association with the pair Cu – Zn. Then, the pair Co – Al is added, and later on, the pair pH – Cd. Finally, the pair Ni – Pb is associated to this second cluster.

A study of the correlation matrix of the analysed parameters, as a step previous to the cluster analysis, could be interesting in order to indicate the degree of relationship between variables and to eliminate parameters that show a low correlation coefficient (Table 4). The toxicity to Microtox shows a good correlation with Fe and sulphate ($r > 0.9$, $\rho<0.05$) and with As and Cr ($r > 0.7$, $\rho<0.05$). On the other hand, high levels of positive correlation among different pairs of variables such as Cu and Zn ($r > 0.9$, $\rho<0.05$), Cd and Cu ($r > 0.7$, $\rho<0.05$) or Al and Cu ($r > 0.6$, $\rho<0.05$) are also observed.

In the light of the results, it can be interpreted the toxicity to Microtox of the sediments is mainly associated to concentrations of Fe, SO_4^{2-}, As and Cr. These concentrations are higher in the sediments from AMD-watercourse. Elements such as Co, Cu, Al and Zn, show higher concentrations in the sediments belonging to Villar Creek after the join. These elements along with the Cd are also directly connected with the pH of the water as the right side of the dendogram shows (Fig. 7). Thus, when the pH increases these elements are found in the most mobile phases of the sediments, increasing their bioavailability.

4. Conclusions

The present study shows that contamination by AMD has an important role in altering the physical, chemical and biological characteristics of a natural stream. Large amounts of metallic ions and sulfate flowing into the uncontaminated stream resulting in the chemical degradation of the stream. Although the concentrations of toxic elements in water decrease along the watercourses, the results show that pollution of AMD is mainly transferred to the sediments of the natural river due to the strong precipitation of iron and aluminum and the cooprecipitation of the rest of the toxic elements on them, increasing their potential toxicity. A natural creek affected by AMD can store a huge amount of pollution in its sediments and exhibits a not very low water pH and low water metal concentration.

According to the different factors used to evaluate the contamination in the studied sediments, it can be considered as strongly polluted sediments due mainly to the high concentrations of Cu and As in the AMD-sediments and by Cu and Zn in the creek sediments. The elevated concentrations of these elements involve an important potential risk on the aquatic environment, associated both in waters and sediments. On the other hand, Microtox test informs that the sediments are extremely or very toxic, associated to concentrations of Fe, SO_4^{2-}, As and Cr for the AMD-watercourse sediments, while Al, Cd, Cu and Zn seem to be liable of the toxicity for the creek sediments.

These results clearly expose that although water contamination is strongly reduced after joining with the unpolluted waters from Villar Creek, the massive metal precipitation on the bedrock of Villar Creek have to be seriously considered as a potential stress to the ecosystems. The different processes observed in this area are widely observed in the Odiel basin and in other basins affected by AMD and therefore the results presented in this study can be extended and applied to the whole Odiel basin and to other basins in the world affected by AMD.

Acknowledgements

This study has been financed by the Spanish Ministry of Science through projects CTM2005-07282-C03-C01/TECNO, CTM2008-06344-C02-C02/TECNO, CTM2008-06344-C02-C03/TECNO and CGL2010-21956-C02-02. A.M.S. was financially supported by the postdoctoral position within the Juan de la Cierva program of the Spanish Government. The comments and helpful criticisms of the Reviewers and the assistance and support of the Executive Editor, Dr. John G. Farmer, have considerably improved the quality of the original manuscript and are gratefully acknowledged

References

Allison J D, Brown D S, Novo-Gradac K J. MINTEQA2/PRODEFA2. A geochemical assessment model for environmental systems. Version 3.0. Environmental Research Laboratory, Office of Research and Development, U.S. Environmental Protection Agency. Athens, Georgia; 1990.

Asta MP, Ayora C, Acero P, Cama J. Fiel rates for natural attenuation of arsenic in Tinto Santa Rosa acid mine drainage (SW Spain). J Hazar Mater 2010b; 177: 1102-1111.

Asta MP, Ayora C, Román-Ross G, Cama J, Acero P, Gault AG, Charnock JM, Badelli F. Natural attenuation of arsenic in the Tinto Santa Rosa acid stream (Iberian Pyritic Belt, SW Spain): The role of iron precipitates. Chem Geol 2010a; 271: 1-12.

AZUR Environmental. Microtox M500 Manual. AZUR Environmental, Carlsbad, CA, USA;1998.

Bennett J, Cubbage J. Review and evaluation of Microtox test for freshwater sediments. Report of the Washington State Department of Ecology, Olympia, Washington; 1992.

Bigham JM, Nordstrom DK. Iron and Aluminum Hydroxysulfates from Acid Sulfate Waters. In: Alpers CN, Jambor JL, Nordstrom DK eds., Sulfate Minerals: Crystallography, Geochemistry, and Environmental Significance. Reviews in Mineralogy and Geochemistry, Mineralogical Society of America., Chantilly, Virginia; 2000. p. 351-403.

Blasco J, Arias AM, Sáenz V. Heavy metals in organisms of the river Guadalquivir estuary: possible incidence of the Aznalcóllar disaster. Sci Tot Environ 1999; 242: 249–259.

Boularbah A, Schwartz C, Bitton G, Morel JL. Heavy metal contamination from mining sites in South Morocco: 1. Use of a biotest to assess metal toxicity of tailings and soils. Chemosphere 2006; 63: 802-810.

Brouwer H, Murphy T, McArdle L. A sediment contact bioassay with Photobacterium phosphoreum. Env Toxicol Chem 1990; 9: 1353-1358.

Campisi T, Abbondanzi F, Casado-Martinez C, DelValls TA, Guerra R, Iacondini A. Effect of sediment turbidity and color on light output measurement for Microtox Basic Solid-Phase Test. Chemosphere 2005; 60: 9-15.

Canovas CR, Hubbard CG, Olias M, Nieto JM, Black S, Coleman ML. Hydrochemical variations and contaminant load in the Rio Tinto (Spain) during flood events. J Hydrol 2008; 350: 25-40

Cánovas CR, Olías M, Nieto JM, Galván L. Wash-out processes of evaporitic sulfate salts in the Tinto river: Hydrogeochemical evolution and environmental impact. Appl Geochem 2010; 25: 288-301

Cánovas CR, Olías M, Nieto JM, Sarmiento AM, Cerón JC. Hydrogeochemical characteristics of the Tinto and Odiel rivers (SW Spain). Factor controlling metal contents. Sci Total Environ 2007; 373: 363–382.

Caraballo MA, Rötting T, Nieto JM, Ayora C. Sequential extraction and DXRD applicability to poorly crystalline Fe- and Al-phase characterization from an acid mine water passive remediation system. Am Mineral 2009a; 94: 1029-1038.

Caraballo MA, Rötting TS, Macías F, Nieto JM, Ayora C. Field multi-step limestone and MgO passive system to treat acid mine drainage with high metal concentrations. Appl Geochem 2009b; 24: 2301-2311.

Delgado J, Sarmiento AM, de Melo MTC, Nieto JM. Environmental Impact of Mining Activities in the Southern Sector of the Guadiana Basin (SW of the Iberian Peninsula). Water Air Soil Poll 2009; 199: 323-341.

Delistraty D, Yokel J. Chemical and ecotoxicological characterization of Columbia River sediments below the Handford site (USA). Ecotox Environ Safe 2007; 66: 16-28.

Grande JA, Andujar JM, Aroba J, de la Torre ML, Beltran R. Precipitation, pH and metal load in AMD river basins: an application of fuzzy clustering algorithms to the process characterization. J Environ Monitor 2005; 7: 325-334.

Grimalt JO, Ferrer M, Macpherson E. The mine tailing accident in Aznalcollar. Sci Tot Environ 1999; 242: 3-11.

Guéguen C, Gilbina R, Pardosa M, Dominika J. Water toxicity and metal contamination assessment of a polluted river: the Upper Vistula River (Poland). Appl Geochem 2004; 19: 153–162.

Hakanson L. An ecological risk index for aquatic pollution control. A sedimentological approach. Water Res 1980; 14: 975-1001.

Imai A, Gloyna EF. Effects of pH and oxidation state of chromium on the behavior of chromium in the activated sludge process. Water Res 1990; 24: 1143– 50.

Kahru A, Pollumaa L, Reiman R, Ratsep A. Microbiotests for evaluation of the pollution from the oil shale industry. In: New Microbiotests for Routine Toxicity Screening and Biomoritoring. Guido Persoone, Colin Janssen, Will De Coen Editors. Kluwer Academic New York 2000. p. 357-365.

Kim MH, Sho YS, Kim EJ, Chung SY, Hong MK. Studies on heavy metal contamination of agricultural products, soils and irrigation waters in abandoned mines, Korea. Food Hyg Safe 2002; 17: 178–182.

Landrum PF, Robbins JA. Bioavailability of sediment-associated contaminants to benthic invertebrates. In: Baudo R, Giesy JP, Muntau H, editors. Sediments: chemistry and toxicity of in-place pollutants. Boca Raton (FL): Lewis Publishers 1990. p. 237– 63.

Mowat FS, Bundy KJ. Correlation of field-measured toxicity with chemical concentration and pollutant availability. Environ Int 2001; 27: 479-489.

Müller G. Die Schwemetallbelastung der sediments des Neckars und seiner Nebenflusse: eine Bestandsanfnahme. Chemical Zeitung 1981; 105: 157– 64.

Olias M, Ceron JC, Moral F, Ruiz F. Water quality of the Guadiamar River after the Aznalcollar spill (SW Spain). Chemosphere 2006b; 62: 213-225.

Olías M, Nieto J M, Sarmiento A M, Cerón J C, Canovas C R. Seasonal water quality variations in a river affected by acid mine drainage: The Odiel river (south west Spain). Sci Tot Environ 2004; 333: 267-281.

Olías M, Cánovas C, Nieto JM, Sarmiento AM. Evaluation of the dissolved contaminant load transported by the Tinto and Odiel rivers (South West Spain). Appl Geochem 2006a; 21: 1733–1749.

Parkhurst DL, Appelo CA J. User´s guide to PHREEQC - A computer program for speciation, reactionpath, 1D-transport, and inverse geochemical calculations. U.S. Geological Survey, Water-Resources Investigations Report 99-4259, 312, 1999.

Peplow D, Edmonds R. The effects of mine waste contamination at multiple levels of biological organization. Ecol Eng 2005; 24: 101–119.

Pérez-López R, Asta MP, Román-Ross G, Nieto JM, Ayora C, Tucoulou R. Synchrotron-based X-ray study of iron oxide transformations in terraces from the Tinto-Odiel river system: Influence on arsenic mobility. Chem Geol 2011; 280: 336-343.

Power EA, Champan PM. Assessing sediment quality. In: Burton GA (ED). Sediment Toxcity Assessment. Lewis Pub, Boca Raton, FL, 1992. p. 1-18.

Riba I, Delvalls TA, Forja J M, Gómez-Parra A. Influence of the Aznalcóllar mining spill on the vertical distribution of heavy metals in sediments from the Guadalquivir estuary (SW Spain). Mar Pollut Bull 2002; 44: 39-47.

Riba I, Casado-Martinez MC, Forja J M, DelValls A. Sediment quality in the Atlantic coast of Spain. Environ Toxicol Chem 2004; 23: 271-282.

Rodier J, Broutin JP, Chambon P, Champsaur H, Rodi L. L’analyse De L’eau. Dunod, Paris 1996.

Roussel C, Bril H, Fernandez A. Arsenic speciation: involvement in evaluation of environmental impact caused by mine wastes. J Environ Qual 2000; 29, 182-188.

Sarmiento AM, Nieto JM, Olías M, Cánovas CR. Hydrochemical characteristics and seasonal influence on the pollution by acid mine drainage in the Odiel river Basin (SW Spain). Appl Geochem 2009a; 24: 697-714.

Sarmiento AM, Nieto JM, Casiot C, Elbaz-Poulichet F, Egal M. Inorganic arsenic speciation at river basin scale: the Tinto and Odiel Rivers in the Iberian Pyrite Belt, SW Spain. Environ Pollut 2009b. 157: 1202-1209.

Sarmiento AM, Oliveira V, Gómez-Ariza JL, Nieto JM, Sánchez-Rodas D. Diel cycles of arsenic speciation due to photooxidation in acid mine drainage from the Iberian Pyrite Belt (SW Spain). Chemosphere 2007; 66, 677-683.

Sarmiento AM. Study of the pollution by acid mine drainage of the surface waters in the Odiel basin (SW Spain). Ph.D. Thesis, Univ. Huelva, Spain. UMI ProQuest, Publ. No.: AAT 3282346. Ann Arbor, USA

2008.<http://proquest.umi.com/pqdweb?did=1404342661&sid=3&Fmt=2&clientId=40400&RQT=309&VName=PQD>

Stronkhorst J, Schipper C, Brils J, Dubbeldam M, Postman J, Van De Hoeven N. Using marine bioassays to classify the toxicity of Dutch Harbor sediments. Environ Toxicol Chem 2003; 22: 1535-1547.

Tyler G, Carrasco R, Nieto JM, Perez R, Ruiz MJ, Sarmiento AM. Optimization of Mayor and Trace Element Determination on Acid Mine Drainage samples by Ultrasonic Nebulizer-ICP-OES (USN-ICP-OES) Pittcon Conf. 7–12 March. Chicago, USA. 2004. 9000/1000.

Van Beelen P. A review on the application of microbial toxicity tests for deriving sediment quality guidelines. Chemosphere 2003: 53, 795-808.

Zanker H, Moll H, Richter W, Brendler V, Hennih C, Reich T, Kluge A, Huttin G. The colloid chemistry of acid rock drainage solution from an abandoned Zn-Pb-Ag mine. Appl Geochem 2002; 17: 633-648.

Figure captions

Fig. 1. Odiel River Basin location map indicating study ubication and sampling points

Fig. 2. Physicochemical parameters measured in the field and several chemical processes occurring along the watercourse.

Fig. 3. Metal distribution in sediment samples according to the bioavailable fractions and non-available fractions

Fig. 4. Evolution of As and Cr species ratios along the watercourse.

Fig. 5. Geoaccumulation indexs along the watercourse for several toxic elements

Fig. 6. Environmental risk factors for the sediment and water samples along the watercourse

Fig. 7. Cluster analysis dendrogram for the data related to the sediment samples, including pH of the water samples, metal and sulphate concentration of the extracted from the most bioavailable fraction (F1) and toxicity test data.

Tables

Table 1. Some metals, metalloids and sulphate dissolved in the water samples

Station	pH	EC	SO_4	Al	Cu	Fe(II)	Fe(III)	Mn	Zn	As	Ba	Cd	Co	Cr	Ni	Pb
		$mScm^{-1}$	$mg\ l^{-1}$							$\mu g\ l^{-1}$						
TR2	3.2	3.2	7884	72	15	645	27	35	64	3764	5.7	104	1096	6.2	832	724
TR3	3.1	3.3	8460	76	19	622	90	37	68	2332	6.0	108	1172	12	864	148
TR4	3.0	3.3	8424	76	19	491	149	36	68	1600	3.4	116	1176	14	872	132
TR5	2.9	3.2	8460	80	20	413	199	37	72	1248	4.1	104	1192	14	900	122
V6	4.8	2.5	1008	7.6	2.3	31	6.2	4.4	8.0	53	15	8.7	128	1.5	84	1.1
V7	5.2	0.6	900	6.0	2.0	29	3.6	3.8	7.2	1.2	17	1.1	116	1.7	76	1.3
V8	6.4	0.5	432	0.1	0.6	8.2	2.6	1.6	2.7	1.2	16	2.3	40	5.4	33	1.1
V1	7.8	0.2	48.4	<dl	0.1	<dl	0.7	0.3	0.4	<dl	13	<dl	11	<dl	4.2	<dl

<dl: below detection limit

Table 2. Contamination factors (C^i_f) for the metals and degree of contamination (C_d) of the sediment samples.

	Contamination factor (C^i_f)							
Metal	**TR2**	**TR3**	**TR4**	**TR5**	**V6**	**V7**	**V8**	Average
As	89.1	187	87.5	68.0	88.0	26.0	16.5	87.5
Cd	6.45	10.7	4.00	2.36	3.77	<0.01	11.3	4.00
Co	0.20	0.08	0.11	0.15	0.06	0.32	0.80	0.15
Cr	0.15	0.13	0.09	0.24	0.06	0.18	0.16	0.15
Cu	24.8	16.8	13.1	17.3	11.0	85.9	203	17.3
Ni	0.39	0.37	0.02	0.22	<0.01	0.41	0.55	0.37
Pb	35.7	12.0	1.41	11.5	0.96	3.40	3.51	3.51
Zn	8.40	8.56	7.60	7.68	7.84	13.8	44.6	8.40
Degree of contamination (C_d)	165	236	114	108	112	130	281	130

Table 3. Microtox EC50 values with 95% confidence limits for sediments along the water course. (Toxic unit: TU=100/EC50).

	EC_{50}			
	mg/L	**95% C.L.**	**%**	**TU**
TR2	783	518-1119	1.29	77.8
TR3	176	104-263	0.29	346
TR4	170	67.0-280	0.28	358
TR5	183	110-301	0.30	332
V6	83.0	67.0-106	0.14	733
V8	210	182-240	0.34	29.0

EC_{50}	Classification[1]
> 2%	Non toxic
1 -2%	Slightly toxic
0.75 - 0.99%	Moderately toxic
0.5 - 0.74%	Toxic
0.25 - 0.49%	Very toxic
0.0 - 0.24%	Extremely toxic

TU	Classification[2]
< 1	Non toxic
1 - 10	Toxic
10 - 100	Very toxic
> 100	Extremely toxic

[1]Brouwer et al., 1990; Bennett and Cubbage, 1992
[2]Kahru et al., 2000

Table 4. Correlation matrix including pH of the water samples, metal and sulphate concentration of the extracted from the most bioavailable fraction (F1) and toxicity test data (TU: Toxic unit)

	TU	As	Cd	Co	Cr	Cu	Ni	Pb	Zn	Al	Fe	pH	SO_4
TU	1												
As	0.77	1											
Cd	-0.39	-0.65	1										
Co	-0.03	0.39	-0.42	1									
Cr	0.66	0.77	-0.65	0.70	1								
Cu	0.06	-0.20	0.66	0.15	0.12	1							
Ni	-0.15	0.33	-0.42	0.42	0.27	-0.28	1						
Pb	-0.68	-0.37	-0.31	0.22	-0.27	-0.60	0.11	1					
Zn	0.26	0.14	0.39	0.39	0.43	0.93	-0.03	-0.68	1				
Al	-0.14	-0.26	0.13	0.58	0.37	0.64	-0.21	0.07	0.60	1			
Fe	0.99	0.70	-0.40	-0.09	0.61	0.01	-0.28	-0.60	0.17	-0.12	1		
pH	-0.14	-0.03	0.65	-0.09	-0.37	0.38	-0.21	-0.30	0.31	-0.20	-0.20	1	
SO_4	0.94	0.83	-0.39	0.27	0.83	0.23	-0.03	-0.68	0.49	0.09	0.90	-0.09	1

Figure 1

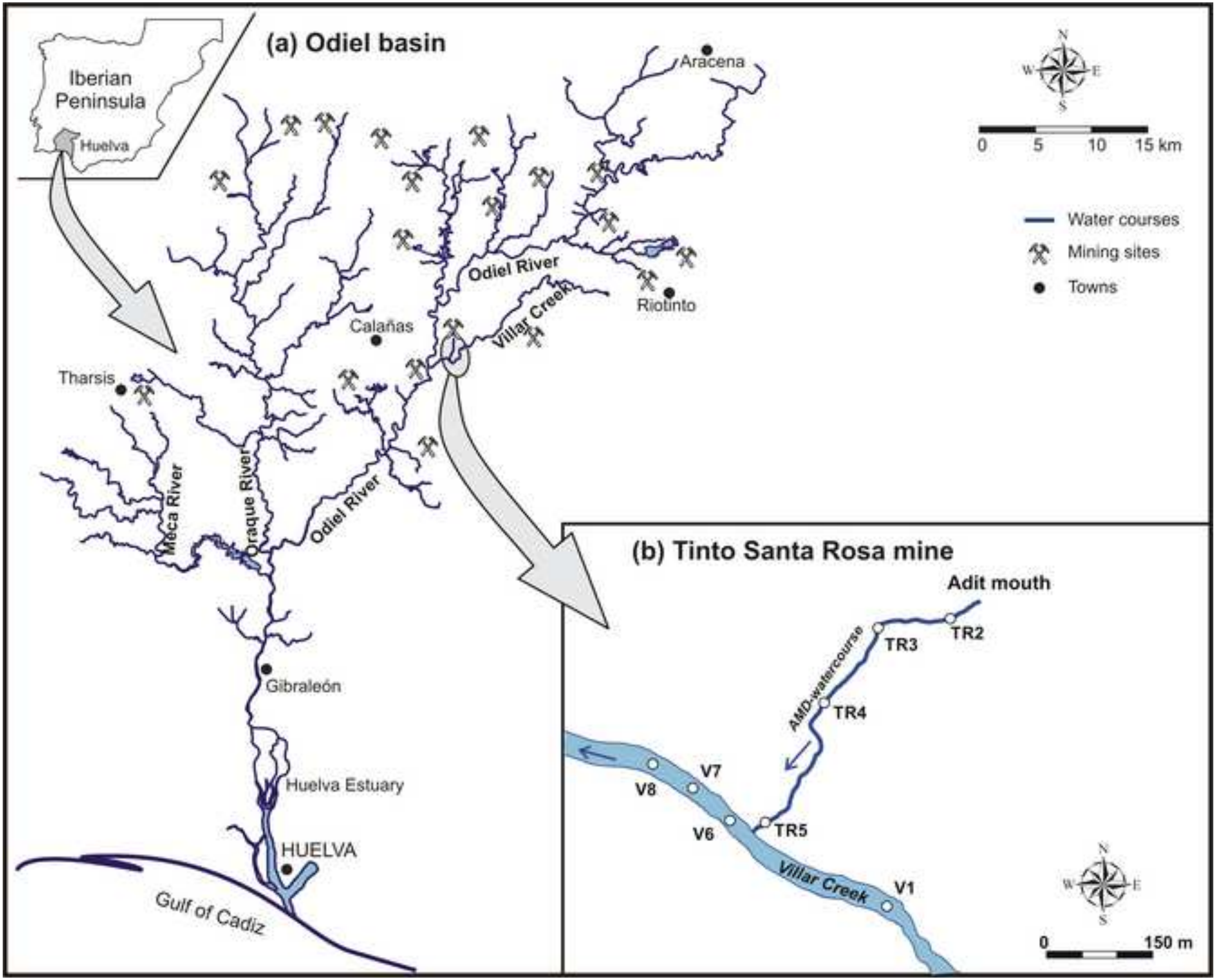
(a) Odiel basin
Iberian Peninsula
Huelva
Aracena
Riotinto
Calañas
Tharsis
Odiel River
Villar Creek
Meca River
Oraque River
Odiel River
Gibraleón
Huelva Estuary
HUELVA
Gulf of Cadiz
0 5 10 15 km
Water courses
Mining sites
Towns
(b) Tinto Santa Rosa mine
Adit mouth
TR2
TR3
AMD-watercourse
TR4
TR5
V1
V6
V7
V8
Villar Creek
0 150 m

Figure 2

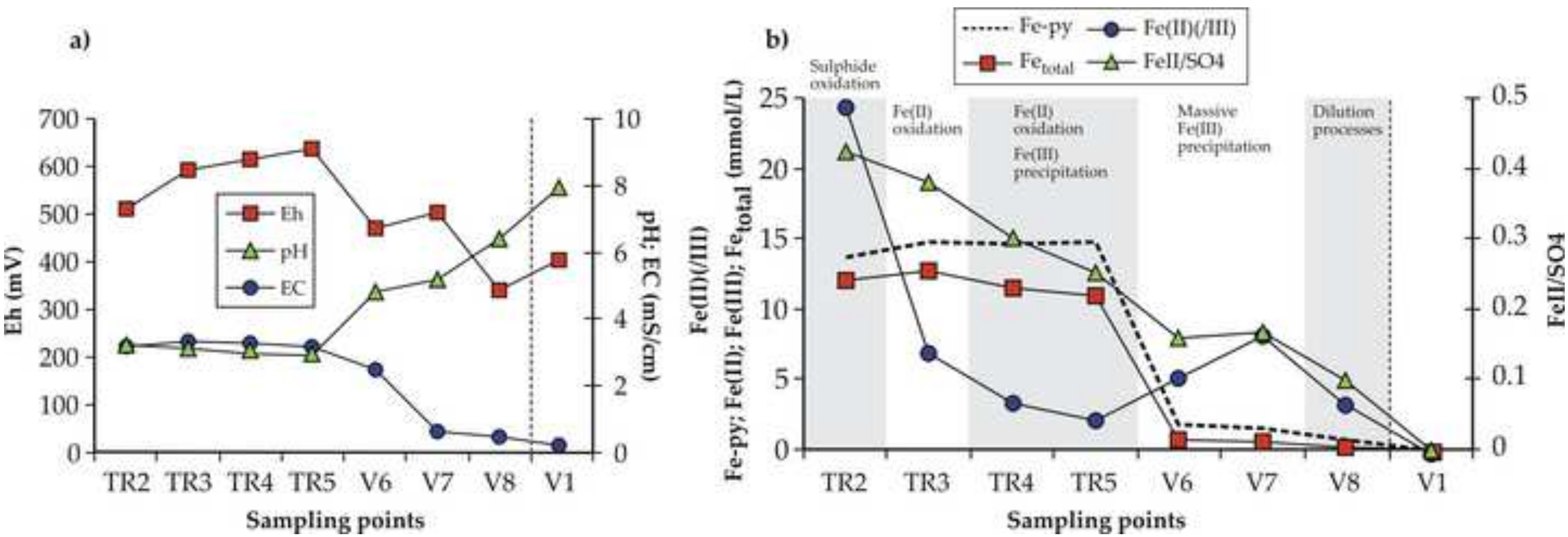

a)
Eh (mV)
pH; EC (mS/cm)
Eh
pH
EC
TR2 TR3 TR4 TR5 V6 V7 V8 V1
Sampling points
b)
Fe-py
Fe(II)(/III)
Fe_total
FeII/SO4
Sulphide oxidation
Fe(II) oxidation
Fe(II) oxidation
Fe(III) precipitation
Massive Fe(III) precipitation
Dilution processes
Fe-py; Fe(II); Fe(III); Fe_total (mmol/L)
Fe(II)(/III)
FeII/SO4
TR2 TR3 TR4 TR5 V6 V7 V8 V1
Sampling points

Figure 3

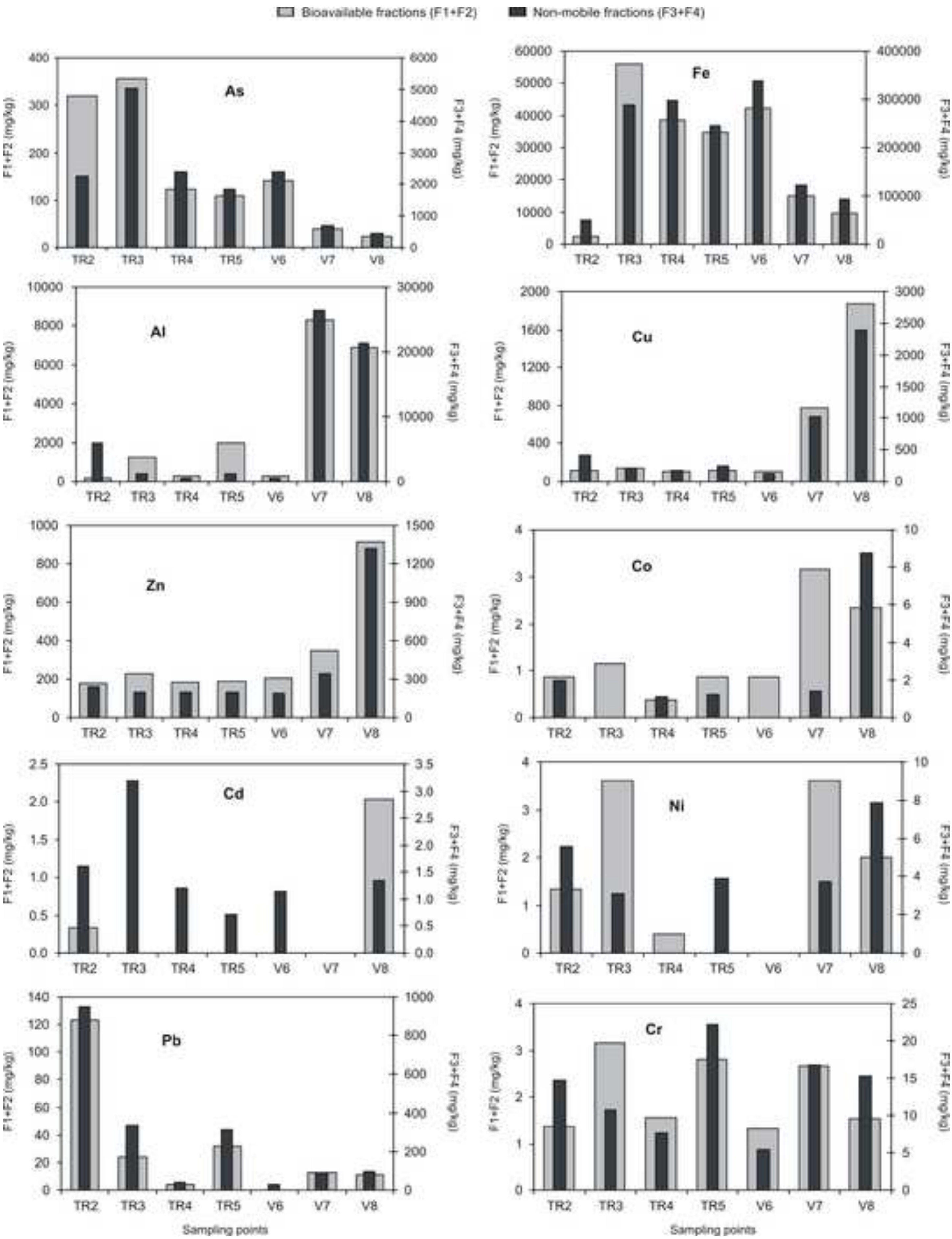

Bioavailable fractions (F1+F2)
Non-mobile fractions (F3+F4)
As
Fe
Al
Cu
Zn
Co
Cd
Ni
Pb
Cr
F1+F2 (mg/kg)
F3+F4 (mg/kg)
TR2 TR3 TR4 TR5 V6 V7 V8
Sampling points

Figure 4

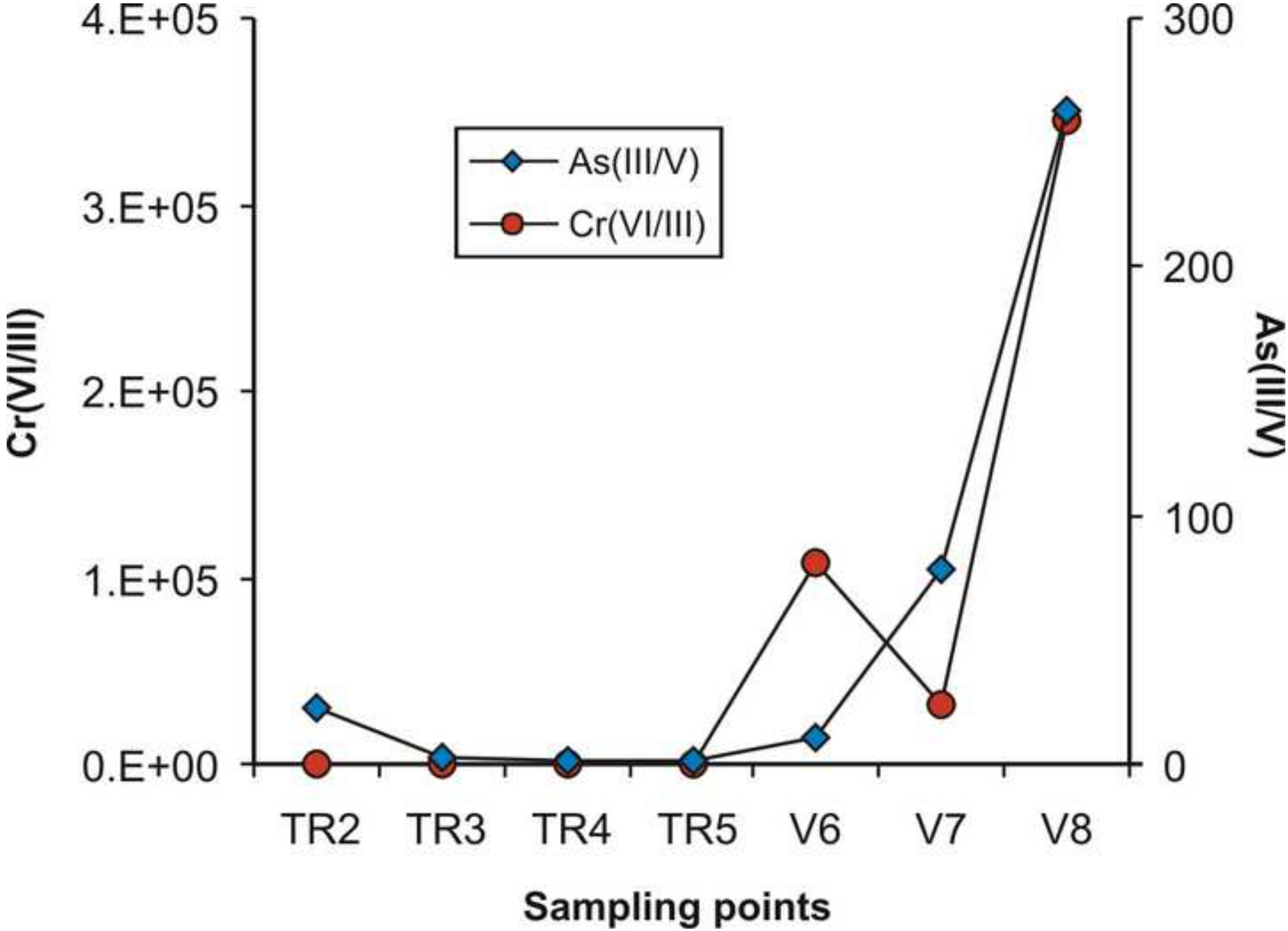
4.E+05
3.E+05
2.E+05
1.E+05
0.E+00
300
200
100
0
Cr(VI/III)
As(III/V)
As(III/V)
Cr(VI/III)
TR2
TR3
TR4
TR5
V6
V7
V8
Sampling points

Figure 5

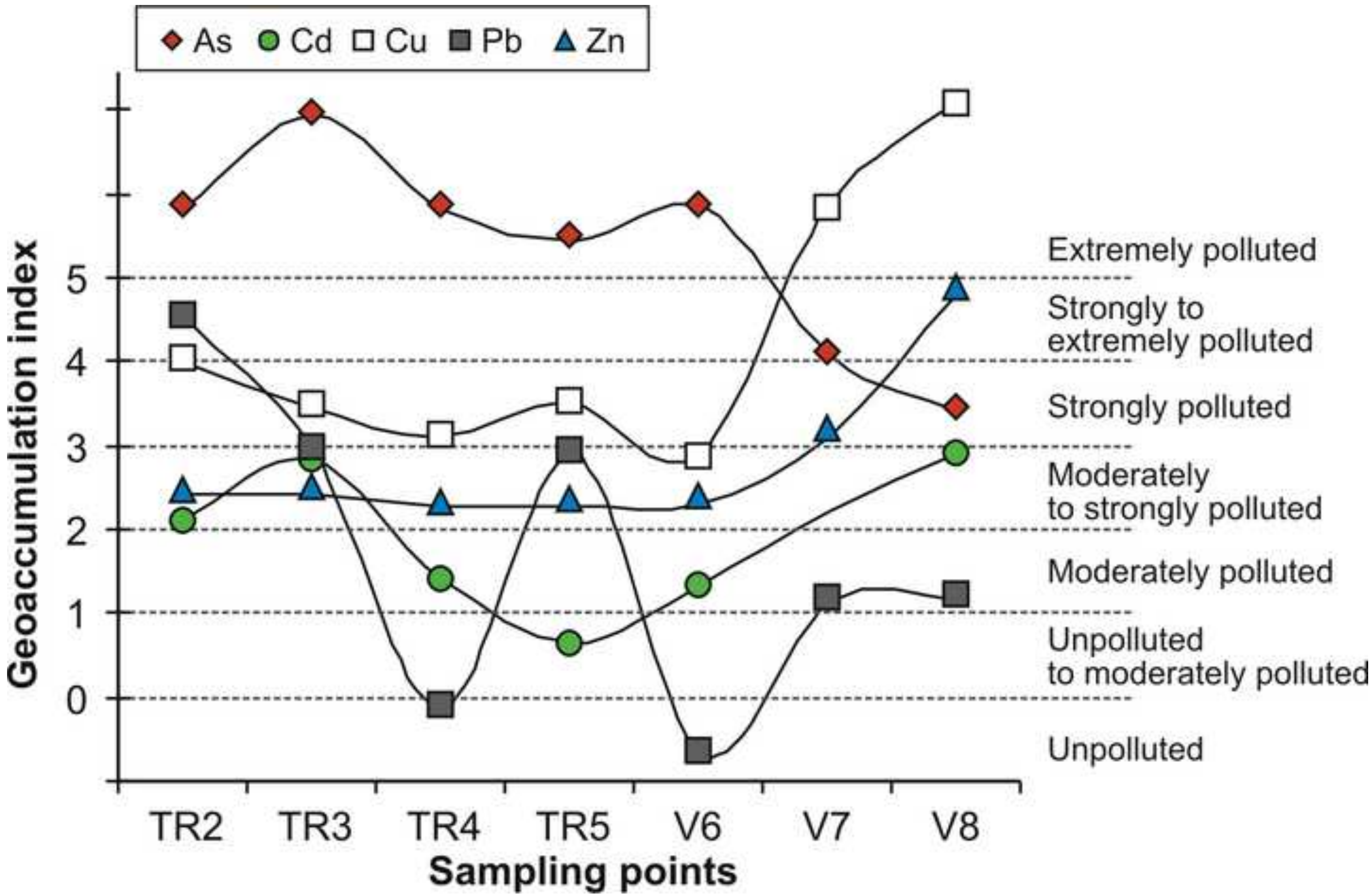

As
Cd
Cu
Pb
Zn
Geoaccumulation index
5
4
3
2
1
0
Extremely polluted
Strongly to extremely polluted
Strongly polluted
Moderately to strongly polluted
Moderately polluted
Unpolluted to moderately polluted
Unpolluted
TR2
TR3
TR4
TR5
V6
V7
V8
Sampling points

Figure 6

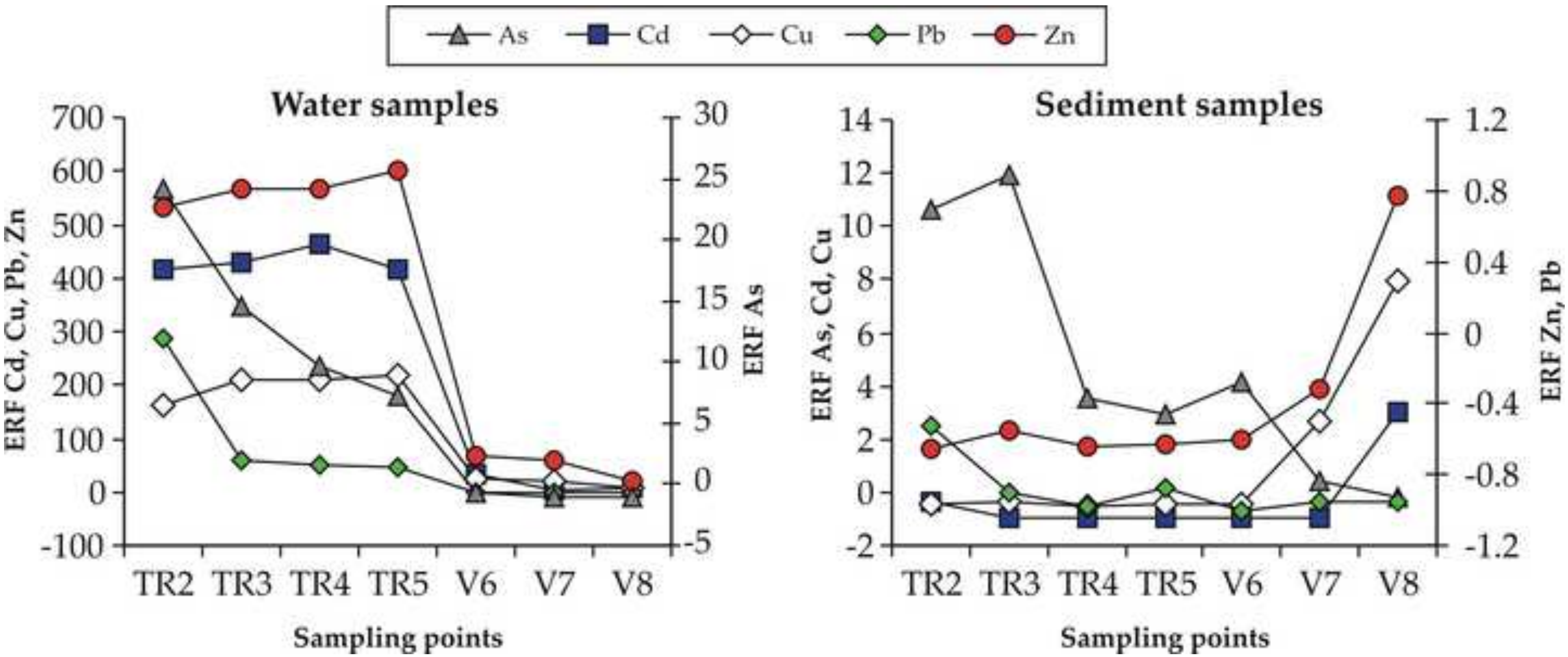
As
Cd
Cu
Pb
Zn
Water samples
ERF Cd, Cu, Pb, Zn
ERF As
700
600
500
400
300
200
100
0
-100
30
25
20
15
10
5
0
-5
TR2
TR3
TR4
TR5
V6
V7
V8
Sampling points
Sediment samples
ERF As, Cd, Cu
ERF Zn, Pb
14
12
10
8
6
4
2
0
-2
1.2
0.8
0.4
0
-0.4
-0.8
-1.2
TR2
TR3
TR4
TR5
V6
V7
V8
Sampling points

Figure 7

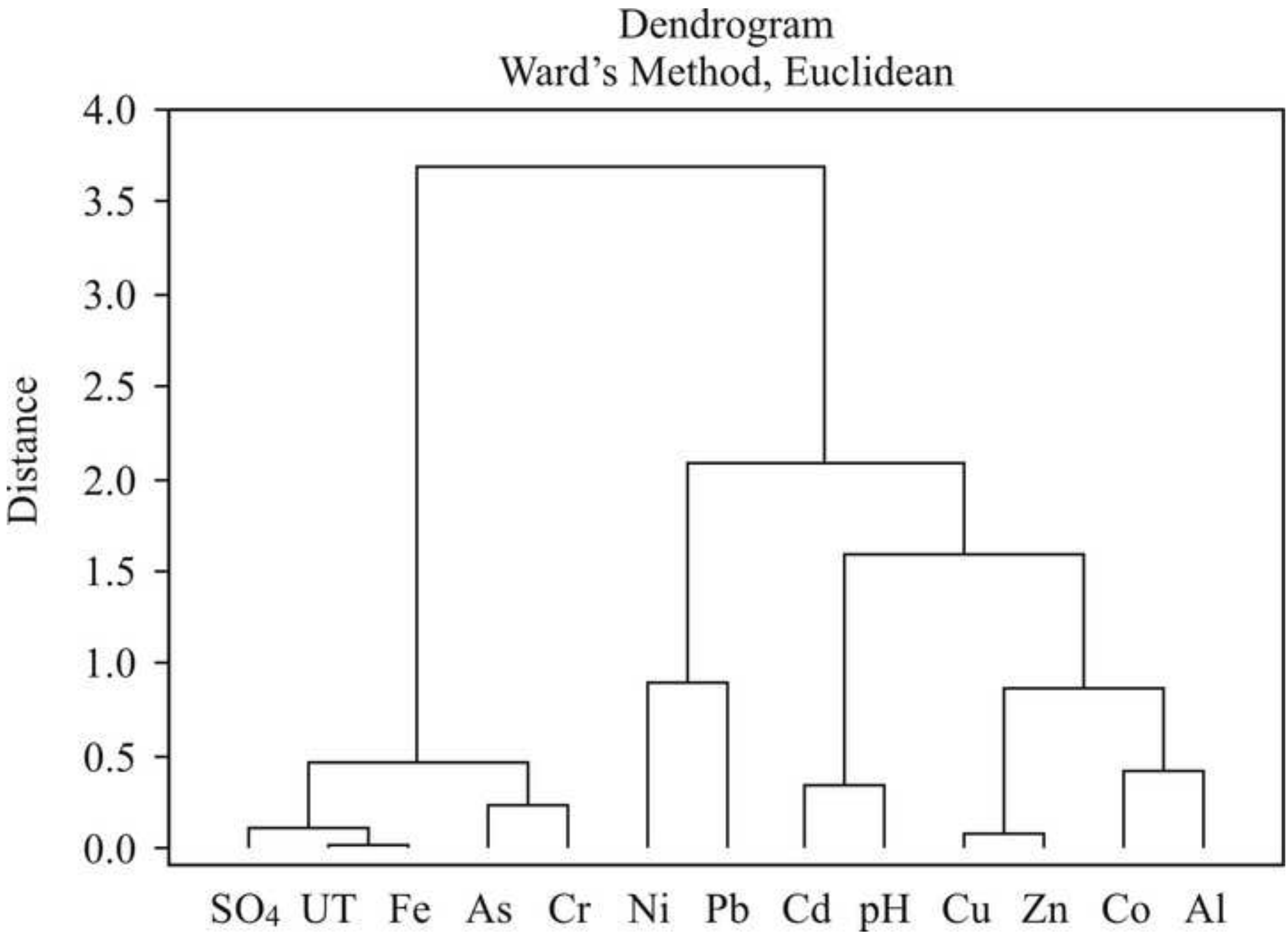
Dendrogram
Ward's Method, Euclidean
4.0
3.5
3.0
2.5
2.0
1.5
1.0
0.5
0.0
Distance
SO4 UT Fe As Cr Ni Pb Cd pH Cu Zn Co Al